Massive MIMO DRA Arrays at Low-frequency Bands for 5G and Beyond

Kerlos Atia Abdalmalak, Ahmed El Yousfi, Daniel Segovia Vargas
(kerlos, ahmed, dani)@tsc.uc3m.es
Department of Signal Theory and Communications, Universidad Carlos III Madrid,
Av. de la Universidad 30, Leganes, Madrid.

***Abstract*—With the advances in 5G, and beyond, mobile communications, more focus is directed toward implementing massive MIMO. While numerous solutions exist for high-frequency bands exceeding 1GHz, exploration of increasing MIMO order in low-frequency bands has not been yet explored, despite their unique characteristics as wide coverage area and penetration through obstacles that are essential for covering a massive number of connected devices. The challenges of designing antenna base station arrays that can support massive MIMO at 5G New Radio (5G NR) 700 MHz bands are summarized. Here, the goal is to move from the current non-massive 4T4R solution to a massive 16T16R MIMO without the increase in the overall size of the base station (restricted to standard sizes) or sacrificing array performance, especially in terms of bandwidth, gain, beamwidth, and isolation. Results based on an array version of differential metallic cap-loaded multi-layer Dielectric Resonator Antenna (DRA) are presented.**

I. Introduction

Future Multiple-Input and Multiple-Output (MIMO) systems aim to increase capacity by introducing more radiating elements to form massive MIMO arrays. These multiple numbers of antennas can narrower the steered beam to optimize the signal at the receiver terminal [1]. Several systems are proposed for higher frequencies, usually higher than 1GHz [2]. However, there is still a big room for enhancement for massive MIMO at the lower band as an essential solution for achieving wider coverage areas and, hence, connecting a massive amount of devices. The challenges of having massive MIMO for 5G, and beyond, base stations at low-frequency bands are devoted mainly to three terms. First, having a compact radiated element, the array can include a larger number of transceivers (TRX) without increasing the total size of the overall system. This also is mandatory for enhancing the isolation between the array elements. Secondly, obtaining a small half-power beamwidth (HPBW) so higher directivity is needed to be able to scan a wide range of angles. And finally, covering broadband to have higher data rates.

To achieve the aforementioned goals several works have been done in recent years. Conventional geometries for wideband dual-polarized antennas that are commonly used for 5G base station applications are proposed such as dipoles [3], patches [4], and slot antennas [5]. However, mostly the size of these antennas is half wavelength or even exceeds it at the working frequency. Therefore the need for developing new compact antennas with broadband radiation is of great importance. Generally, miniaturization can be achieved by inserting meandering lines in patches [6], loading Complementary Split Ring Resonator (CSRR) monopole [7], or high permittivity dielectric resonator [8]. The latter technique is used in designing many dual-polarized compact antennas for massive MIMO 5G base station applications [9]. Although the size is reduced, the main issue of such designs is their narrow bandwidth ($< 5\%$), and low gain. To widen the bandwidth with a compact size and a relatively high gain, a dual-polarized dielectric resonator magneto-electric antenna loaded with a metallic loop [10] is proposed which leads to an improved bandwidth of 14.5% and a gain of $7\,\mathrm{dBi}$. Even though the antenna exhibits a compact size of $0.33\lambda \times 0.33\lambda$, there is still room for enhancing both the bandwidth and compactness of the radiating element. Another way to achieve broadband is based on loading the metasurface with DRA to form a hybrid system in which two close resonant frequencies are excited, one associated with the DRA whereas the other one is due to the metasurface. As a result, a broad bandwidth of typically 17% [11] and 15.5% [12] is achieved, but at the expense of the large size of $0.5\lambda \times 0.5\lambda$ [11].

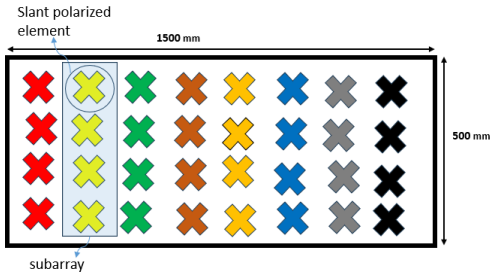

Fig. 1. Architecture of the proposed massive MIMO 5G base station array at low band.

The relatively big size of previous works makes their integration in massive MIMO array scenarios (Fig. 1) a very challenging task when working at the low-frequency band. To implement four dual slant radiating elements in the vertical column of $500\,\mathrm{mm}$ to form a subarray, a compact antenna is needed at $700\,\mathrm{MHz}$. The rest of the paper is organized as follows: Sec. II presents the element design of the massive antenna array based on a differential metallic cap-loaded multi-layer Dielectric Resonator Antenna (DRA). The results of the array configuration are discussed in Sec. III while the main conclusions are drawn in Sec. IV.

II. Compact broadband single radiating element

As a summary of the previous section, to implement massive MIMO at low-frequency bands with the same current size restrictions of base stations, the main requirements for the antenna element are

- Bandwidth: covering broadband from $700\,\mathrm{MHz}$ to $800\,\mathrm{MHz}$

- Polarization: dual slant linear polarization ($\pm 45°$).
- Size: Compact element with a size smaller than $0.23\lambda_{fmin} \times 0.23\lambda_{fmin}$ which is corresponding to $100\,\text{mm} \times 100\,\text{mm}$ for a minimum frequency of $700\,\text{MHz}$.
- Gain: high gain above $6\,\text{dBi}$ to produce a smaller HPBW.
- Height: low profile smaller than $0.23\lambda_{fmin}$ which is corresponding to $100\,\text{mm}$.

After testing several radiation elements, the section provides the best-optimized element that covers these requirements.

A. Differential metallic cap-loaded multi-layer DRA element

As concluded from the previous discussions, the main challenge for massive MIMO base stations at low frequency is how to make the dual-polarization element compact while keeping the broadband, high gain, good radiation patterns antenna performance. From the perspective of miniaturized and compact antennas, DRA can be a solution to that goal whenever it overcomes its inherent associated problems such as its extremely low bandwidth and gain performance that makes it less attractive for many broadband applications. DRAs have the ability to provide a very compact design by using high permittivity. Materials with very high permittivity up to $\epsilon_r = 140$ are commercially available [13]. For example, high values ($\epsilon_r > 35$) could provide elements with compact lengths smaller than 0.1λ, however, at the same time, the bandwidth is usually very small (lower than 5%) [8]. Hence bandwidth enhancement techniques are needed, several methods, can be used to offer broadband DRA, for example, tapered strip excitation [14] enables broadband but the gain is small, also, stair-shaped multi-layer [15], although it requires an increase in overall size which is not preferable here.

After studying different broadband enhancement methods and their effects on other antenna parameters, multi-layer DRA with a fixed size and multiple materials [16] provide the best performance. It is based on exciting different modes and controlling them to form a broadband solution. However, the bandwidth is still not wide enough, therefore the addition of a metallic cap [17] covering the top layer is proposed as presented in Fig. 2. The metallic cap at the top almost cancels the frequency-dependence of the excited mode on the resonator height making broadening BW achievable by increasing the height. Finally, differential feeding is used which provides higher BW compared to normal coaxial or microstrip feeding.

Using High-frequency Simulation Software (HFSS), the reflection coefficient is depicted in Fig. 3, it shows that this solution covers from $680\,\text{MHz}$ to $830\,\text{MHz}$ (20%) which is slightly larger than the band under interest. This is achieved with a very compact dielectric element with a total size of $37\,\text{mm} \times 37\,\text{mm} \times 80\,\text{mm}$ ($0.08\lambda_{fmin} \times 0.08\lambda_{fmin} \times 0.18\lambda_{fmin}$. The DRA element consists of three blocks whose bottom and top layers are made of material with $\epsilon_r = 35$ while the middle layer has a permittivity of $\epsilon_r = 50$. Both materials are available via several dielectric resonator suppliers [13]. Our previous studies demonstrated that compact DRA designs can be achieved with lower relative permittivity but to preserve good performance you need to modify the shape such as using more complex shapes [18] or changing

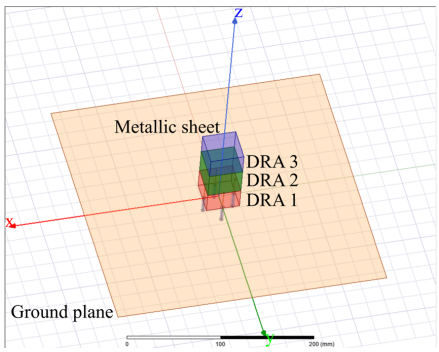

Fig. 2. Dual-polarized differential metallic cap-loaded multi-layer DRA element.

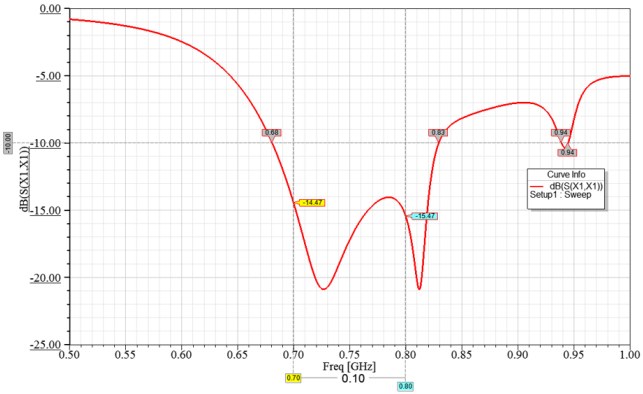

Fig. 3. S_{11} of the differential metallic cap-loaded multi-layer DRA.

aspect ratios [19]. This proposed element provides perfectly symmetric patterns for both dual $\pm 45°$ polarization and for all ϕ cut planes. As an example, the radiation patterns at one cut plane are plotted for 700 and $800\,\text{MHz}$ in Fig. 4. It has pure polarization discrimination with a Cross Polar Discrimination (XPD) greater than $50\,\text{dB}$ and a good Front to Back Ratio (FBR) level above $11\,\text{dB}$. Additionally, it offers a completely flat gain of $6.5\,\text{dBi} \pm 0.2$ with an almost constant HPBW of $86 \pm 2°$.

III. MIMO ANTENNA ARRAY

From the discussion of Section II and considering the whole size restriction of the base station, compact elements are needed to implement massive MIMO and be able to fit eight subarrays which each subarray is a quadruplet consisting of four elements. Hence, the requirements for the subarray can be summarized as

- Number of radiators: 64 ($32\times$ dual-polarization) elements in the form of 16 subarrays ($8\times$ dual-polarization) which each consist of 4 elements.
- Size: each subarray is $0.44\lambda_{fmin} \times 1.17\lambda_{fmin}$ which is corresponding to $187\,\text{mm} \times 500\,\text{mm}$ for a minimum frequency of $700\,\text{MHz}$.
- HPBW: Smaller vertical HPBW of about 30 to $35°$.
- Isolation: good isolation between subarrays lower than $20\,\text{dB}$.

A. DRA array

In this section, an array based on the proposed differential metallic cap-loaded multi-layer DRA of Section II-A will

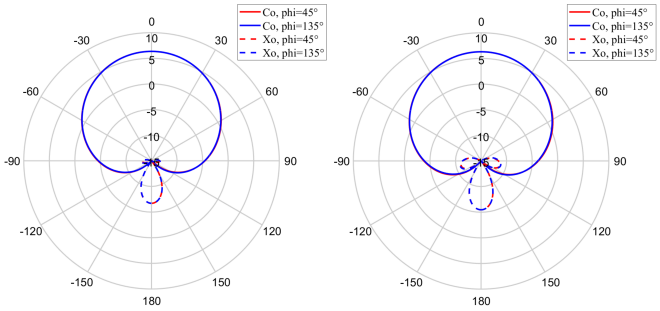

Fig. 4. Radiation patterns of dual-polarized differential metallic cap-loaded multi-layer DRA at (a) 700MHz and (b) 800MHz.

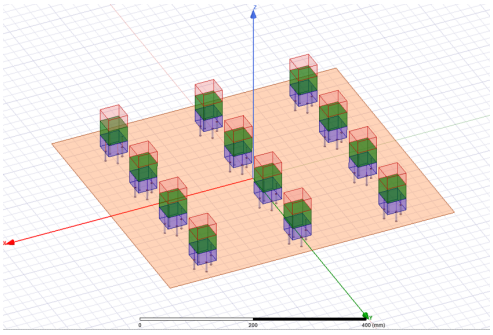

Fig. 5. A dual-polarized three quadruplet subarrays based on differential metallic cap-loaded multi-layer DRA.

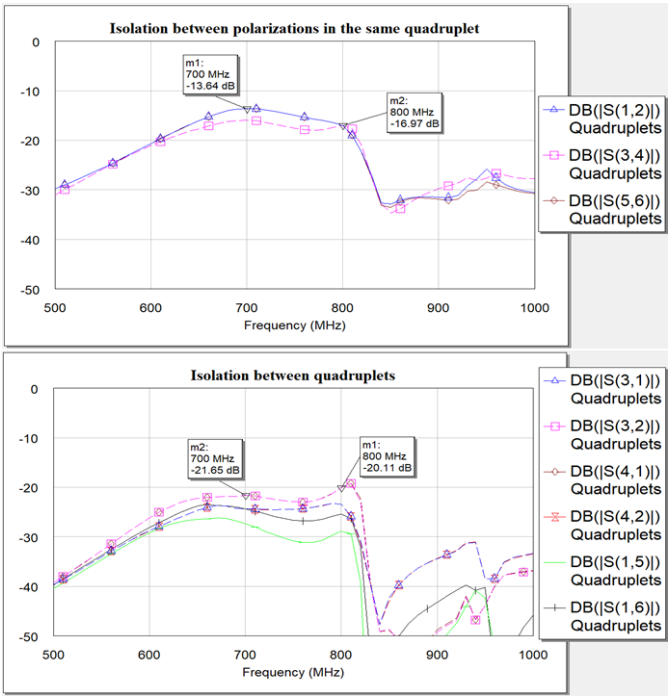

Fig. 6. Isolation S_{ij} between polarization S_{11} (top) and between different subarrays (bottom) of the three 4-element DRA subarrays.

be analyzed. A truncated version of the complete array will be considered, consisting of three dual-polarized subarrays (instead of eight in the full version) as presented in Fig. 5. This reduces the computational time while considering all the electromagnetic interactions between the neighbor's subarrays are taken into account, as well as the edge effects. To completely fulfill the massive MIMO requirements in terms of size, the spacing between elements is $(125\,\mathrm{mm})$ to fit the four elements in the $500\,\mathrm{mm}$ vertical side $(1.17\lambda_{700MHz})$ while the subarrays are setting $187.5\,\mathrm{mm}$ apart from each other to fit the eight subarrays in the required size of $1500\,\mathrm{mm}$ $(1.17\lambda_{700MHz})$ for the horizontal side. With this truncated version, the complete effects in the array can be studied such as the performance of edge subarrays and mutual coupling for the internal subarrays without the need to run the extensive simulation for the complete MIMO system. Besides the ability to measure isolation between neighbor subarrays in terms of first and second-neighbor interaction while no need to test for other farther neighbors as their coupling will be negligible.

For each polarization, the two differential feedings are connected through a balun to ensure the same amplitude with a $180°$ phase shift between them. Then the output of the balun is connected to one leg of 4×1 combiner/power divider. The same is repeated for each element, then the output of the combiner/power divider forms the final port for this subarray at this polarization. So, in this truncated version, the full-wave simulation for the 12 dual-polarized elements is performed in HFSS using 48 separated ports, then the 48×48 s-parameters are exported in the form of *.s48p file. Finally, this file is imported to Applied Wave Research (AWR) microwave Office software where the 48 ports are connected through 24 baluns then six 4×1 combiners/power dividers to provide the final six output ports where each subarray has two ports one for $-45°$ and other for $+45°$ polarization. It is worth mentioning that the losses for this corporate feeding are about 1 to 2 dB, however, as the focus here is on the radiator itself, ideal feeding networks are used in AWR.

The three subarrays present almost the same reflection coefficients S_{ii} with a high level of coherence between external and internal subarrays for both polarizations and a good matching level below $-14\,\mathrm{dB}$ in the band of interest from 700 to $800\,\mathrm{MHz}$. The isolation between polarizations in the same subarray is below $-16\,\mathrm{dB}$ and $-13.5\,\mathrm{dB}$ for internal and external subarrays respectively at the lower frequencies (Fig. 6) with an enhancement at higher ones. Indeed, the isolation value is relatively weak which is mainly because of the high mutual coupling between polarizations due to their very small spatial separation (lower than $\lambda \div 10$ in the whole band). On the contrary, the isolation between subarrays (which is the more relevant for the MIMO systems) is excellent being lower than $-20\,\mathrm{dB}$ in the whole band. Also, for the second-neighbor interaction such as S_{15} and S_{16}, the level is already negligible which confirms that no need to study farther neighbors and three subarrays are enough to check the performance for the complete array without the need to test the full eight subarrays.

From the point of view of radiation characteristics, Fig. 7 summarizes the behavior in the form of the gain as a function of the frequency of both co-polar and cross-polar components. For simplicity and due to the high symmetry, the results are shown for a single polarization and a single subarray (the middle one). The solid and dashed lines mark the co-polar and cross-polar components respectively. As expected from the robust performance of the proposed element and the almost constant HPBW that was presented in Fig. 4, the

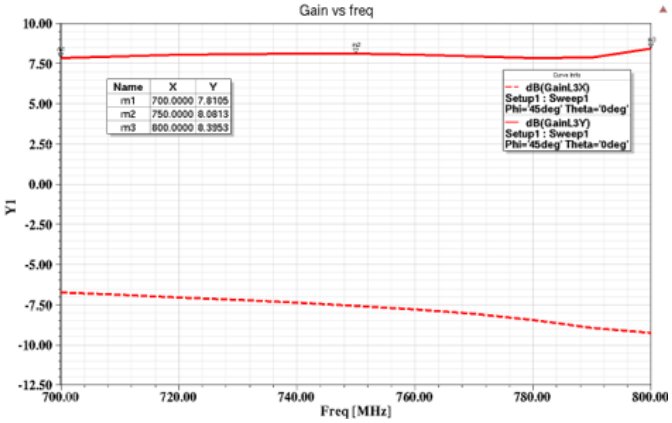

Fig. 7. Gain vs frequency of the three 4-element DRA subarrays.

array's HPBW at both vertical and horizontal planes provide good results for all subarrays (curves are omitted here due to the size restriction). The subarray reduces the vertical HPBW from 86 (for the element) to narrow HPBW of 32° and 36° at 800 MHz and 750 MHz respectively, the small changes are due to the change of the element spacing in terms of electric length with a slight increase to 38° at the lower band of 700 MHz. For the horizontal plane, the subarray has an almost fixed HPBW of $117 \pm 2°$. The subarray has an almost flat gain of 8.1 ± 0.3 dBi with XPD and FBR above 15 dB and 13 dB over the band under interest respectively.

Overall, we can see that this array satisfies most of the massive MIMO requirements, especially in terms of the size where the 16T16R dual-polarized elements can fit in the base station.

IV. Conclusions

The main challenges and requirements for designing a massive MIMO antenna in both element and array levels are investigated. A compact array element of a dual-polarized DRA antenna based on multi-layer and metallic cap-loading is presented as a suitable candidate for future massive MIMO base stations. It provides a compact size of $(0.08\lambda_{fmin} \times 0.08\lambda_{fmin})$ and still covers a wide enough band of about 20% from 680 MHz to 830 MHz. This is in addition to a flat high gain of 6 dBi and symmetric radiation patterns with excellent properties.

A truncated version of three subarrays based on this element is studied carefully where each subarray consists of four of the proposed DRA elements. The array covers the complete band from 700 to 800 MHz with excellent levels of matching and isolation between subarrays below -14 dB and -20 dB respectively. Also, it has an almost flat gain of 8.1 ± 0.3 dBi with an average HPBW of 35°. This work can be extended too to include the double number of elements to increase further the MIMO order as eight elements can be fit in each subarray enabling the base station to carry 128 elements (64×dual-polarized) making the total number of elements in the base station. Up to the authors' knowledge, this could not be achieved yet using other solutions at this low-frequency band.

Acknowledgements

We want to thank HUAWEI Technologies Düsseldorf GMBH, Germany for the productive meetings we had and the innovative ideas raised related to antenna design. This work was supported by PID2019-109984RB-C41. Also, Kerlos Atia Abdalmalak wants to thank "Ministerio de Ciencia, Innovación y Universidades" and "Convocatoria de la Universidad Carlos III de Madrid de Ayudas para la recualificación del sistema universitario español" for supporting the Margarita Salas grant and the finance from the European Union - Next Generation EU.

References

[1] S. Aerts, L. Verloock, M. Van Den Bossche, D. Colombi, L. Martens, C. Törnevik, and W. Joseph, "In-situ measurement methodology for the assessment of 5g nr massive mimo base station exposure at sub-6 GHz frequencies," *IEEE Access*, vol. 7, pp. 184 658–184 667, 2019.

[2] E. G. Larsson, T. L. Marzetta, H. Q. Ngo, and H. Yang, "Antenna count for massive mimo: 1.9 GHz vs. 60 GHz," *IEEE Communications Magazine*, vol. 56, no. 9, pp. 132–137, 2018.

[3] Y. Qin, L. Zhang, C.-X. Mao, and H. Zhu, "A compact wideband antenna with suppressed mutual coupling for 5g mimo applications," *IEEE Antennas and Wireless Propagation Letters*, vol. 22, no. 4, pp. 938–942, 2023.

[4] Y. Jin and Z. Du, "Broadband dual-polarized f-probe fed stacked patch antenna for base stations," *IEEE Antennas and Wireless Propagation Letters*, vol. 14, pp. 1121–1124, 2015.

[5] Y. Cui, Y. Niu, Y. Qin, and R. Li, "A new high-isolation broadband flush-mountable dual-polarized antenna," *IEEE Transactions on Antennas and Propagation*, vol. 66, no. 12, pp. 7342–7347, 2018.

[6] A. Lamkaddem, A. E. Yousfi, K. A. Abdalmalak, V. G. Posadas, and D. Segovia-Vargas, "Circularly polarized miniaturized implantable antenna for leadless pacemaker devices," *IEEE Transactions on Antennas and Propagation*, vol. 70, no. 8, pp. 6423–6432, 2022.

[7] A. El Yousfi, A. Lamkaddem, K. A. Abdalmalak, and D. Segovia-Vargas, "A miniaturized triple-band and dual-polarized monopole antenna based on a csrr perturbed ground plane," *IEEE Access*, vol. 9, pp. 164 292–164 299, 2021.

[8] A. Petosa and A. Ittipiboon, "Dielectric resonator antennas: A historical review and the current state of the art," *IEEE Antennas and Propagation Magazine*, vol. 52, no. 5, pp. 91–116, 2010.

[9] X.-Y. Wang, S.-C. Tang, L.-L. Yang, and J.-X. Chen, "Differential-fed dual-polarized dielectric patch antenna with gain enhancement based on higher order modes," *IEEE Antennas and Wireless Propagation Letters*, vol. 19, no. 3, pp. 502–506, 2020.

[10] Z.-Y. Zhang and K.-L. Wu, "A wideband dual-polarized dielectric magnetoelectric dipole antenna," *IEEE Transactions on Antennas and Propagation*, vol. 66, no. 10, pp. 5590–5595, 2018.

[11] Z. Wang, Y. Dong, Z. Peng, and W. Hong, "Hybrid metasurface, dielectric resonator, low-cost, wide-angle beam-scanning antenna for 5g base station application," *IEEE Transactions on Antennas and Propagation*, vol. 70, no. 9, pp. 7646–7658, 2022.

[12] S.-K. Zhao, N.-W. Liu, Q. Chen, G. Fu, and X.-P. Chen, "A low-profile dielectric resonator antenna with compact-size and wide bandwidth by using metasurface," *IEEE Access*, vol. 9, pp. 29 819–29 826, 2021.

[13] K. Luk and K. Leung, *Dielectric Resonator Antennas*, ser. Antennas S. Research Studies Press, 2003.

[14] M. Khalily, M. K. A. Rahim, and A. A. Kishk, "Bandwidth enhancement and radiation characteristics improvement of rectangular dielectric resonator antenna," *IEEE Antennas and Wireless Propagation Letters*, vol. 10, pp. 393–395, 2011.

[15] W. Huang and A. Kishk, "Compact dielectric resonator antenna for microwave breast cancer detection," *IET microwaves, antennas & propagation*, vol. 3, no. 4, pp. 638–644, 2009.

[16] W. W. Huang and A. Kishk, "Compact wideband multi-layer cylindrical dielectric resonator antennas," *IET Microwaves, Antennas & Propagation*, vol. 1, pp. 998–1005(7), 2007.

[17] L. A. Shaik, C. Saha, S. Arora, S. Das, J. Y. Siddiqui, and A. K. Iyer, "Bandwidth control of cylindrical ring dielectric resonator antennas using metallic cap and sleeve loading," *IET Microwaves, Antennas & Propagation*, vol. 11, no. 12, pp. 1742–1747, 2017.

[18] A. E. Yousfi, K. Atia Abdalmalak, A. Lamkaddem, and D. S. Vargas, "Miniaturized broadband dual-polarized dielectric resonator antenna using characteristic modes," in *2023 17th European Conference on Antennas and Propagation (EuCAP)*, 2023, pp. 1–4.

[19] K. A. Abdalmalak, et al., "Microwave radiation coupling into a WGM resonator for a high-photonic-efficiency nonlinear receiver," in *2018 48th European Microwave Conference (EuMC)*, 2018, pp. 781–784.